Borys Bednarek, Tomasz Kik

The Ultrasonic Test-Based Detectability of Cavities in Joints Made of Aluminium Alloys

Abstract: The primary objective of the study involved determining the Phased Array technique-based detectability of internal gas pores in aluminium joints. The test agenda included the making of joints containing artificial discontinuities, the experimental adjustment of test parameters, the performance of tests using a selected testing technique and the comparison of test results with actual dimensions of defects located in metallographic specimens.

Keywords: Non-Destructive Testing, NDT, Ultrasonic Testing, Phased Array

DOI: *10.17729/ebis.2023.1/1*

Introduction

Fatal accidents taking place during the second industrial revolution, such as the explosion of a steam boiler in the Fales & Gray factory of railway cars in Hartford, drew public's attention to numerous imperfections of the then-metallurgy and manufacturing processes. The necessary implementation of additional control measures became obvious, where one of possible solutions involved the detection of defects using methods based on physical phenomena (e.g. the so-called oil and whiting method). The aforesaid measures constituted germs of today's non-destructive tests, yet it was only in the second half of the 20th century that such methods were standardised on an international basis [1].

The development of metallurgy entailed the use of new materials, partly contributing to the implementation of many changes in standards concerning tests of finished products, including welded joints. Previously applied steel grades yielded to new, non-ferrous, materials (e.g. aluminium and its alloys) which better satisfied design-related assumptions and the production of which has been incessantly stimulated by growing demands of transport and food industries. Welded joints made of aluminium are, on a mandatory basis, subject to non-destructive tests, yet in cases of crucial structures (ship hulls, pressure vessels etc.), the above-named tests may prove insufficient to ensure appropriate workmanship. Because of the fact that volumetric tests significantly increase the detectability of hazardous internal defects, the development of appropriate aluminium-related testing methodology should become a priority [2, 3].

Issues concerning ultrasonic tests of welded joints made of aluminium are related to physical properties of the aforesaid metal and their effect on the propagation of ultrasonic waves. Other important problems include the detectability and measurability of typical imperfections located in aluminium joints such as cracks or incomplete fusion. Flaw detectors (defectoscopes) used in the TOFD (i.e. *Time of Flight Diffraction*) and PA (i.e. *Phased Array*) techniques enable the application of many process variables and, consequently, the control of ultrasonic waves within a wide range. The scope of work should include both the experimental adjustment of sets of parameters as well as the measurement of previously generated imperfections and comparing the latter with the actual state, thus making it possible to identify the usability of ultrasonic techniques in tests of aluminium joints [1].

mgr inż. Borys Bednarek – Łukasiewicz – Górnośląski Instytut Technologiczny, Centrum Spawalnictwa (Łukasiewicz Research Network – Upper Silesian Institute of Technology, Welding Research Centre)

dr inż. Tomasz Kik – Politechnika Śląska, Wydział Mechaniczny Technologiczny, Katedra Spawalnictwa (Silesian University of Technology, Faculty of Mechanical Engineering, Department of Welding)

Welding imperfections in aluminium joints

Because of certain specific properties of aluminium, some welding imperfections tend to occur more often in welded joints made of this metal. Imperfections having the greatest impact on the strength and service conditions of welded joints include the following [3–5]:

- hot cracks,
- cavities,
- incomplete fusion.

Significant shrinkage accompanying solidification may trigger the formation of significant deformations in welded joints. The aforesaid phenomenon reduces the dimensional accuracy of structures, yet, in contrast with the above-presented imperfections, it is usually easily visible (detectable) and can be removed. Cavities, incomplete fusion and cracks lead to the significant concentration of stresses, thus translating into potentially dangerous damage to joints. For this reason, the improved detectability of such imperfections is a priority [3–5].

Scope of tests

The research work discussed in the article aimed at the experimental identification of a set of parameters enabling the inspection of welded joints of previously assumed thicknesses. Afterwards, identified parameters were used to verify the detectability of imperfections typical of aluminium joints in previously prepared welds. Results obtained in the tests were compared with actual dimensions, which, in turn, made it possible to assess the effectiveness of the tests.

The implementation of previously adopted assumptions involved the performance of the following agenda:

1. preparation of an aluminium test plate,
2. experimental adjustment of parameters and the selection of a testing technique,
3. preparation of welded joints containing imperfections (gas pores),
4. performance of radiographic tests involving the welded joints,
5. tests of the joints using a previously developed set of parameters,
6. preparation of metallographic specimens sampled from the test joints,
7. performance of microscopic metallographic tests.

Test material

Both the standard plate and all the test welded joints made of aluminium alloy PA11 (EN AW-5754) were characterised by high fatigue strength and corrosion resistance both in an industrial atmosphere and seawater as well as by high arc method-based weldability and machine workability. The above-presented features make aluminium alloy PA11 a popular material in the shipbuilding as well as in the chemical and food industries, where it is used to make pressure vessels, boilers, pipeline elements and pneumatic conduits [3].

The chemical composition and properties of the test material are presented in Tables 1 and 2.

Table 1. Chemical composition of aluminium alloy PA11 [6]

Chemical element		Volume content, %	
		minimum	maximum
Magnesium	Mg	2.6	3.6
Manganese	Mn	-	0.5
Chromium	Cr	-	0.3
	Mn+Cr	0.1	0.6
Silicon	Si	-	0.4
Iron	Fe	0.4	-
Copper	Cu	-	0.1
Zinc	Zn	-	0.2
Titanium	Ti	-	0.15
Aluminium	Al	balance	

Table 2. Properties of aluminium alloy PA11 [6]

Property	Value
Density, g/cm^3	2.68
Melting point, °C	595
Tensile strength R_m, MPa [1)]	220–270
Conventional yield point $R_{0.2}$, MPa [1)]	130
Post-rupture extension A_{50}, % [1,2)]	10
Modulus of longitudinal elasticity E, MPa [1)]	70,500
Modulus of transverse elasticity G, MPa [1)]	26,500
Hardness, HBS [1)]	63
[1)] Hardening state H22 in accordance with EN 485-2:2016 [2)] Specimen thickness t = 10 mm	

Ultrasonic flaw detector

Both the adjustment of parameters and the testing of joints were performed using a testing unit (Fig. 1) composed of the following elements:

- MX2 digital flaw detector,
- HST-Lite scanner,

- 5L32-A31 Phased Array probe,
- power supply units and cables.

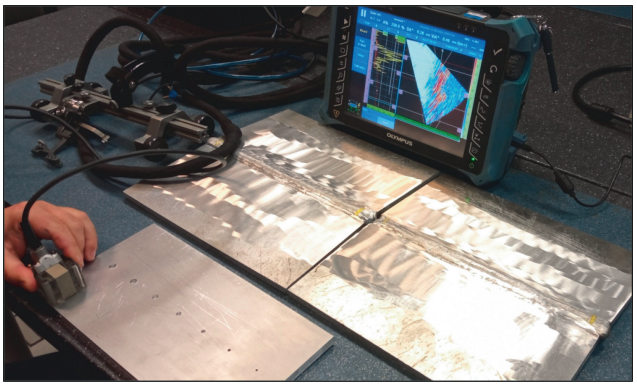

Fig. 1. Ultrasonic testing unit

The OmniScan MX2 flaw detector is a universal unit compatible with more than 10 ultrasonic testing modules (including conventional, TOFD and PA ones). The device features an intuitive interface and many additional functions configurable within a wide range as well as enabling the digital recording of data. The above-named defectoscope is used both in manual and automated tests. The lightweight and robust housing of the device enables its operation in laboratories, industrial shops and under field conditions [7].

Table 3 presents selected flaw detector parameters.

Table 3. Parameters of the OmniScan MX2 flaw detector [7]

Parameter	Value
Bandwidth, MHz	0.6–18
Aperture [1)]	32
Number of elements [1)]	128
Group size [1)]	up to 8 elements
Imaging modes [1)]	linear, sectoral
Refresh rate, Hz [1)]	60
[1)] Values related to the Phased Array module	

Experimental adjustment of parameters

The process of parameter adjustment started with preparing the stand and cleaning the standard specimen (in accordance with the PN-EN ISO 16811:2014-06 and PN-EN ISO 18563-1-3 standards, Fig. 2). The probe was connected to the defectoscope, whereas the test surface was wetted with water (coupling agent). The configuration of input data is presented in Table 4. In turn, results concerning TCG function parameter values are presented in Table 5.

Table 4. Configuration of input data

Parameter	Value
Test material	Aluminium
Plate thickness, mm [1)]	10
Wave angular range, °	40–72
Angle resolution, °	1
Number of elements used in the test	16
Beam configuration	sectoral
Shear wave velocity, m/s	3,240
Longitudinal wave velocity, m/s	6,300
[1)] Equivalent to joint thickness	

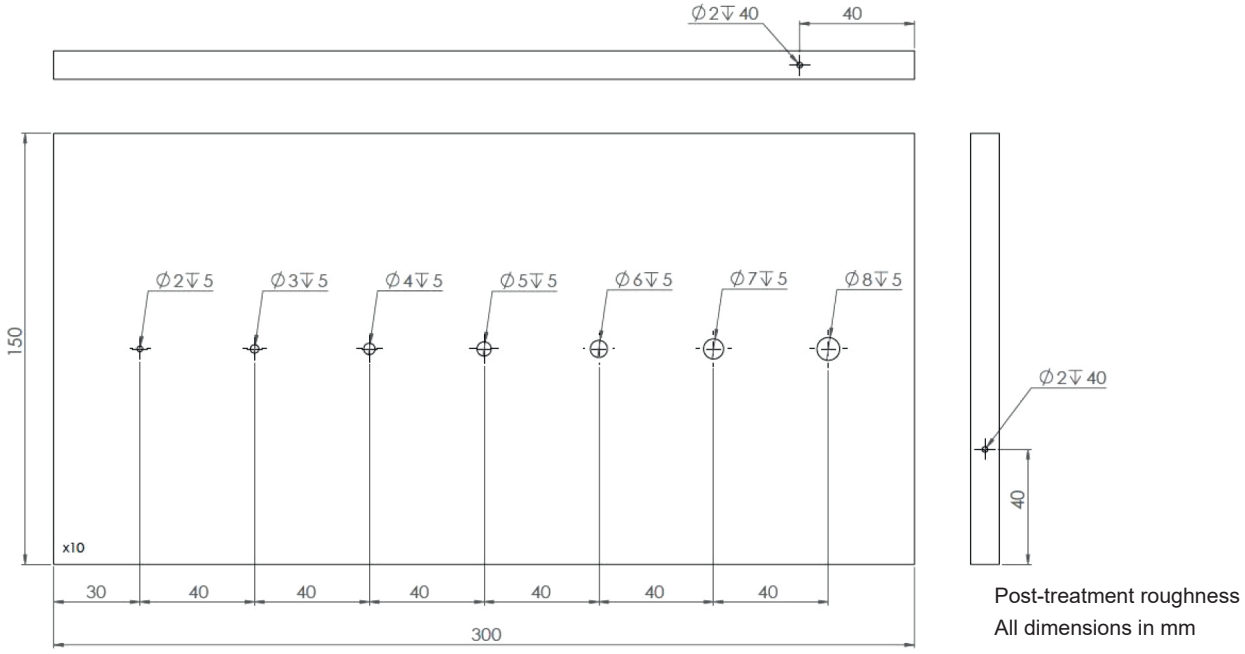

Fig. 2. Production drawing of the standard plate

Table 5. Parameters of TCG function points

TCG point	Position, mm	Value of compensation gain, dB	Amplitude without compensation, dB
1	0	0	22
2	3.60	2.1	19.9
3	11.81	7.2	14.8
4	20.56	12.3	9.7
5	28.59	16.1	5.9
6	37.12	20.5	1.5
Initial gain – 22 dB			

Welding of aluminium joints

The pre-weld preparation of 10 mm thick plates involved the bevelling of the edges at an angle of 45° as well as cleaning the latter using an alcohol solution and lint-free cloth. The generation of imperfections required the covering of interpass surfaces with a small amount of paraffin oil. The process parameters are presented in Table 6.

Table 6. Welding process parameters

Parameter	Joint		
	no. 1	no. 2	no. 3
Welding method	MIG (131)		
Type of current	DC (+)		
Current, A	185		
Voltage, V	26		
Shielding gas	100% Ar		
Gas flow rate, l/min	8	16	
Filler metal	filler metal wire AlMg4.5, d = 1.2 mm		
Filler metal wire feed rate, m/min	11		

The joints were X-rayed 48 hours after the completion of the welding process. The X-ray process parameters are presented in Table 7.

Table 7. X-ray process parameters

Parameter	Value
X-ray tube acceleration voltage, kV	75
Anode current, mA	5
Time of exposure, min	8

Ultrasonic tests of welded joints

The tests of the welds were performed using the stand prepared for the calibration of the unit. Similar to the previous tests, the coupling medium was water; parameters corresponded to those determined during the adjustment process. The joints were subjected to the grinding process, aimed to remove spatter precluding the smooth movement of the probe on the test surface.

The radiograms were used to identify the probable nature of imperfections in the joint as well as to select areas to be subjected to accurate measurements, aimed to compare the results with the values obtained in the microscopic tests. The process was performed using the previously prepared test stand; the test results are presented in Table 8.

Table 8. Measurement results

No.[1)]	Type of imperfection	Distance from the zero point, mm	Depth, mm	Height, mm
2.1	Gas pore	5.4	1.32	0.91
2.2	Localised porosity	16.81	1.04	2.76
2.3	**Gas pore**	**23.11**	**2.17**	**0.89**
2.4	Gas pore	41.27	4.38	1.03
2.5	Localised porosity	68.92	1.71	3.06
2.6	**Gas pore**	**91.16**	**3.53**	**0.77**
2.7	Crack	110.12	2.25	1.01
2.8	Localised porosity	171.58	1.88	2.14
2.9	**Localised porosity**	**234.91**	**4.01**	**1.97**
2.10	**Gas pore**	**263.4**	**3.15**	**0.72**
3.1	Gas pore	22.07	6.21	0.9
3.2	**Gas pore**	**35.52**	**0.78**	**0.68**
3.3	Localised porosity	44.26	2.05	2.7
3.4	Localised porosity	54.33	1.83	1.01
3.5	Localised porosity	63.71	2.49	3.55
3.6	**Gas pore**	**87.24**	**0.32**	**0.92**
3.7	**Gas pore**	**112.9**	**3.07**	**0.96**
3.8	**Localised porosity**	**133.87**	**0.81**	**2.77**
3.9	Localised porosity	157.43	2.06	4.15
3.10	Gas pore	181.95	1.69	1.27
3.11	Gas pore	197.39	2.12	0.88
3.12	Localised porosity	236.64	3.75	1.26

[1)] The first numeral refers to the joint, where a given defect was verified, whereas the second numeral is the ordinal number

Microscopic tests

The making of metallographic specimens involved weld areas containing large discontinuities in the form of longitudinal and spherical pores (detected

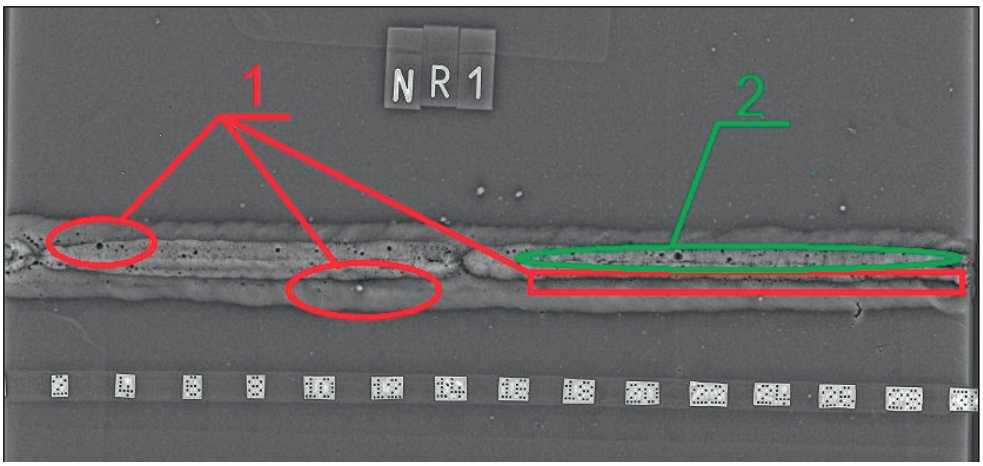

Fig. 3. Radiogram of joint no. 1 – visible incomplete fusion (1) and a crack (2)

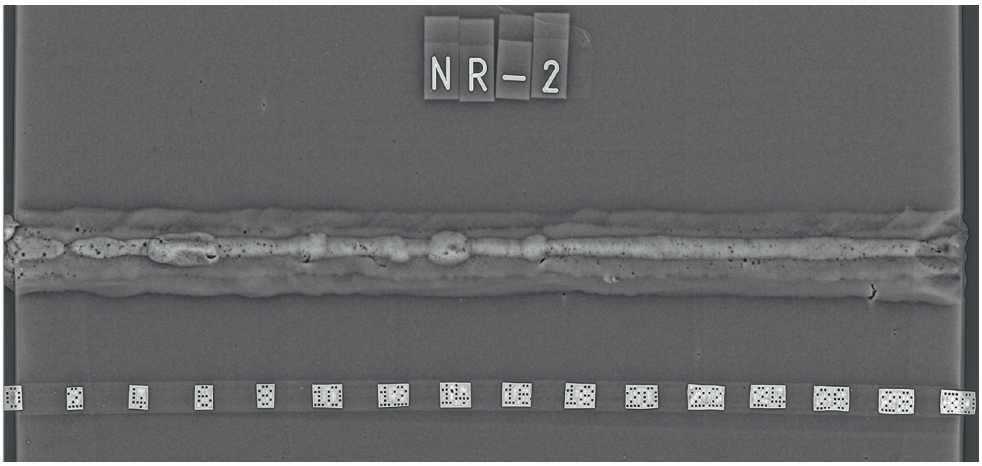

Fig. 4. Radiogram of joint no. 2

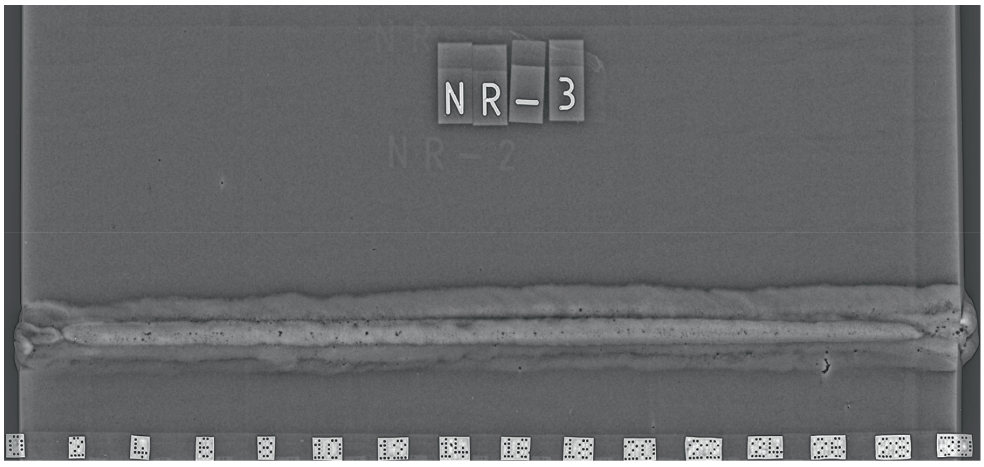

Fig. 5. Radiogram of joint no. 3

during radiographic and ultrasonic tests). The discontinuities were located on both sides of the specimens. The appropriately described joints were subjected to cutting with a band saw.

The tests aimed to identify pore dimensions necessary to determine the effectiveness of the ultrasonic tests. The magnification applied during the tests (amounting to 50×) should enable the performance of sufficiently accurate measurements. Detected imperfections were photographed (Fig. 8) and measured (Table 9) using a dedicated microscope software programme.

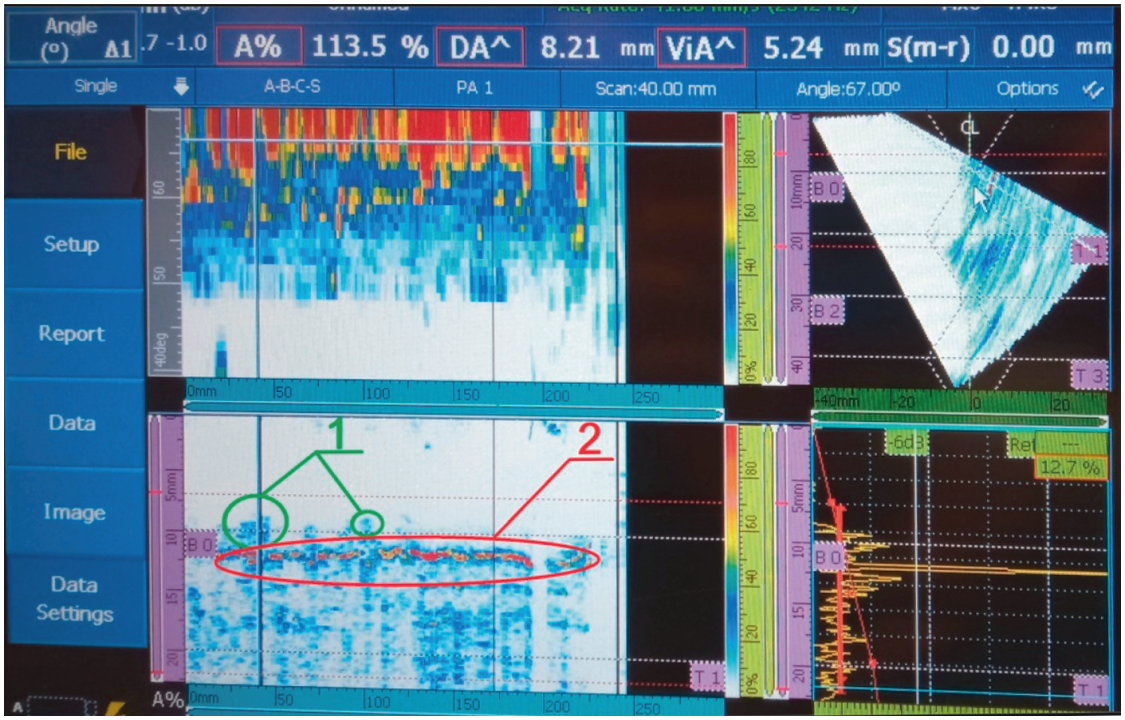

Fig. 6. Test of joint no. 2 – localised porosity (1) and indication generated by the weld root (2)

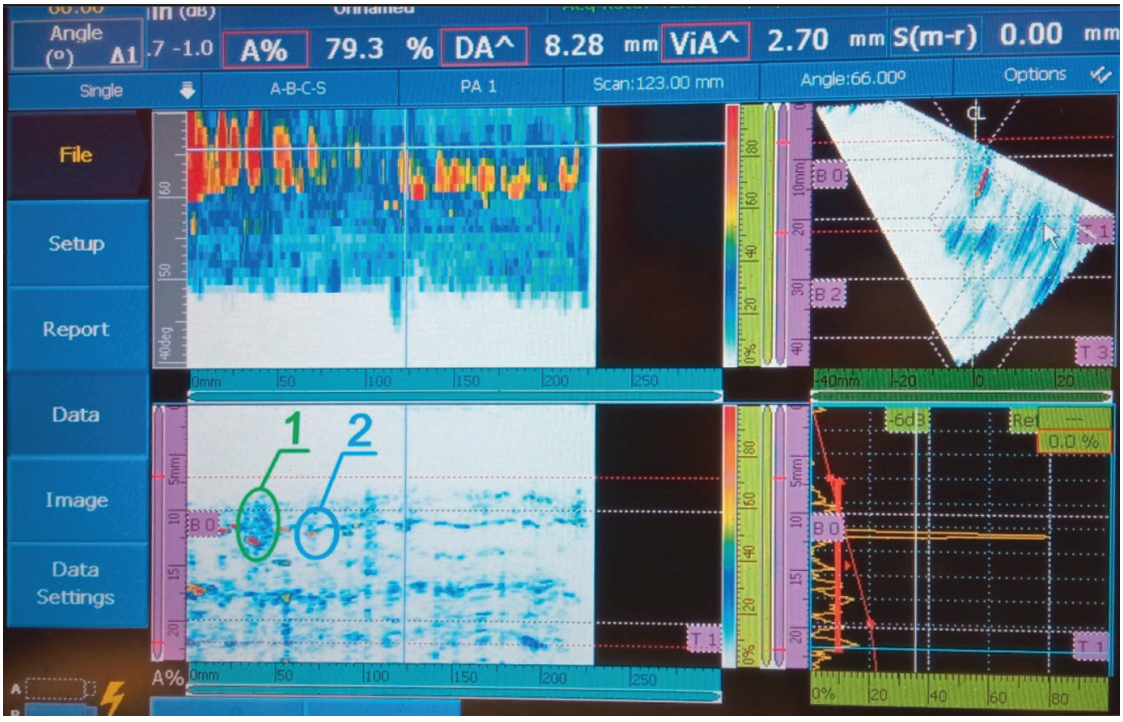

Fig. 7. Test of joint no. 3 – localised porosity (1) and single gas pore (2)

Tables 10 and 11 present the results obtained in the ultrasonic tests confronted with those measured in the specimens. However, the comparison contained in the aforesaid tables does not include indications generated by localised porosity as it was impossible to compare single gas pores from localised porosity with the echo generated by the entire group.

Figures 9 and 10 present the percentage differences between depth and height-related measurement results.

The results obtained in the tests revealed that the depth-related values were similar; the average difference did not exceed 8%, whereas partial differences did not exceed 8.5%. The only exception was the difference related to imperfection no. 5

Table 9. Values measured in metallographic tests

No.[1)]	Type of imperfection	Distance from the zero point, mm	Depth, mm	Height, mm
2.1.1	Gas pore	23	2.01	0.65
2.2.1	Gas pore	91	3.84	0.92
2.2.2	Crack	110	2.12	1.07
2.3.1	Gas pore (one of localised porosity)	235	3.59	0.88
2.3.2	Gas pore (one of localised porosity)	235	3.97	0.54
2.3.3	Gas pore (one of localised porosity)	235	4.19	0.61
2.3.4	Gas pore	263	3.22	0.83
3.4.1	Gas pore	38	0.92	0.59
3.4.2	Gas pore	87	0.27	0.96
3.5.1	Gas pore	112	3.11	0.65
3.5.2	Gas pore (one of localised porosity)	133	0.73	1.38
3.5.3	Gas pore (one of localised porosity)	133	2.08	1.74
3.6.1	Gas pore	178	5.05	0.73
3.6.2	Gas pore (one of localised porosity)	197	1.75	0.52
3.6.3	Gas pore (one of localised porosity)	197	2.23	0.79
3.6.4	Gas pore (one of localised porosity)	197	3.06	0.31

[1)] First numeral refers to the number of a given joint, the second numeral refers to the number of a given specimen, where imperfections were verified, whereas the third numeral is the ordinal number

(amounting to 18.5%), which was connected with a shallow depth at which the imperfection was located. The weld face, located directly above the imperfection, generated its own echo, thus disturbing the process of measurement. It was not possible to notice an explicit tendency related to differences between the methods. In relation to certain discontinuities, depths estimated using the ultrasonic technique were greater than those identified during the metallographic tests (and vice versa).

The tests results concerning imperfection heights were also similar, yet, in the aforesaid case differences were significant. The highest partial difference reached nearly 48%. However, it should be noted that the values obtained in the measurements were low, which means that measuring them by means of the Phased Array technique was more difficult. Similar to the depth measurements, the comparison of height-related measurements did not reveal the existence of an explicit tendency related to differences between the testing methods.

The height of most of the gas pores measured using the ultrasonic method exceeded 0.5 mm. In the above-presented case, the detection of individual pores of similar or smaller primary dimensions was impeded by the overly low impulse amplitude. The application of higher amplitude was characterised by certain restrictions related to the number and nature of the remaining imperfections, yet such an approach should be taken into account in cases of welding methods and conditions creating the risk related to the dissolution of the excessive amount of gases in the liquid metal.

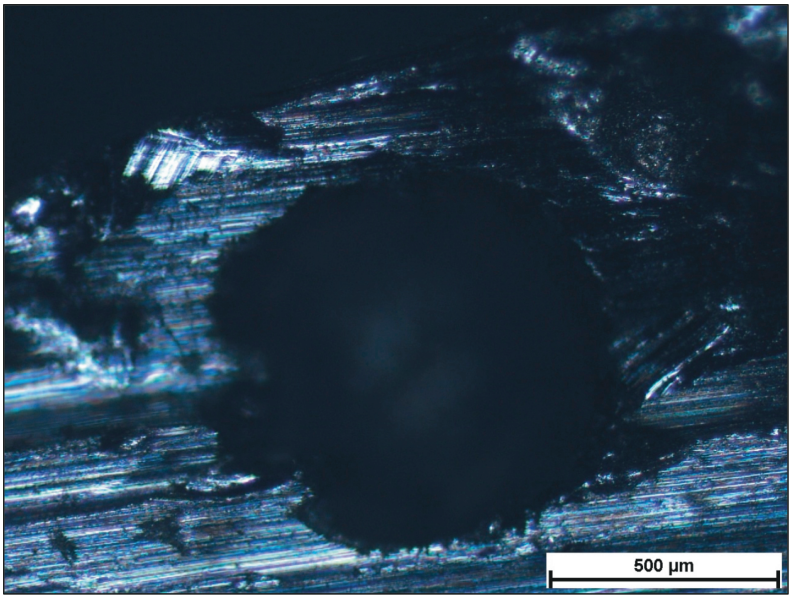

Fig. 8. Gas pore in specimen no. 4

Table 10. Comparison of test results (indication depth)

No.	Distance from the zero point, mm	Measured value, mm		Statistical values		
		PAUT	Micro.	Average	Range	Relative error, %
1	23 (joint no. 2)	2.17	2.01	2.09	0.16	7.9
2	91 (joint no. 2)	3.53	3.84	3.69	0.31	8.07
3	110 (joint no. 2)	2.25	2.12	2.19	0.13	6.13
4	263 (joint no. 2)	3.15	3.22	3.19	0.07	2.17
5	87 (joint no. 3)	0.32	0.27	0.3	0.05	18.5
6	112 (joint no. 3)	3.07	3.11	3.09	0.04	1.3

Table 11. Comparison of test results (indication height)

No.	Distance from the zero point, mm	Measured value, mm		Statistical values		
		PAUT	Micro.	Average	PAUT	Micro.
1	23 (joint no. 2)	0.89	0.65	0.77	0.24	36.92
2	91 (joint no. 2)	0.77	0.92	0.85	0.15	16.3
3	110 (joint no. 2)	1.01	1.07	1.04	0.06	5.61
4	263 (joint no. 2)	0.72	0.83	0.78	0.11	13.25
5	87 (joint no. 3)	0.92	0.96	0.94	0.04	4.17
6	112 (joint no. 3)	0.96	0.65	0.81	0.31	47.69

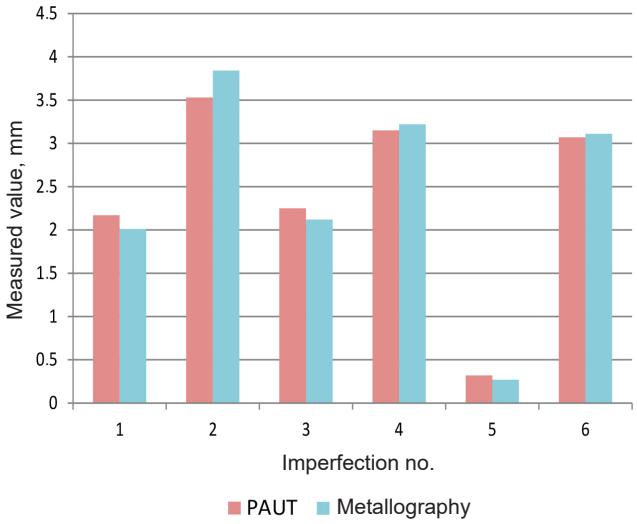

Fig. 9. Comparison of measurement results concerning imperfection depths

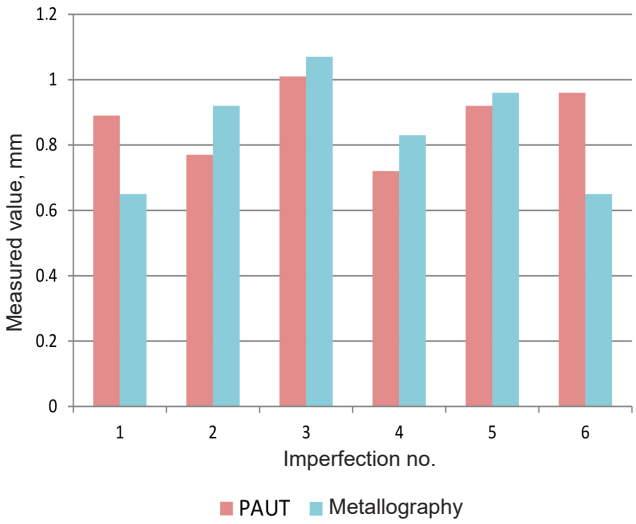

Fig. 10. Comparison of measurement results concerning imperfection heights

Concluding remarks

The research process was performed in accordance with previously adopted assumptions. The results obtained in the tests justified the formulation of the following conclusions:

1. The set of parameters developed during the process of calibration enabled the effective testing of aluminium joints.
2. The Phased Array ultrasonic technique made it possible to effectively detect and measure the depth and height of gas pores located in various areas of welds in aluminium joints. However, the effectiveness was limited by testing parameters as well as dimensions and the location of pores in relation to other cavities and imperfections.
3. The Phased Array technique did not reveal the explicit correlation between the size of gas pores and the accuracy of their measurements.

4. Gas pores located in subsurface layers were characterised by poor detectability, which could be ascribed to the strong echo generated by the weld face and root.

Further research

In terms of the previously adopted objectives, the tests ended successfully, whereas their results could serve as the point of departure for the gradual development of the above-presented scope of knowledge. Further research should aim to confirm obtained information, determine tendencies in research processes and extend the range of materials subjected to tests by including other aluminium alloys, among other things, those with zinc or copper. The growing interest in the subject discussed in the article translates into the high research potential of related issues and inspires further investigation.

References

[1] Pilarczyk J. (edit.): Poradnik inżyniera. Spawalnictwo, T. 1. Wydawnictwa Naukowo-Techniczne, Warszawa 2003.
[2] Szkliniarz W. (edit.): Nowoczesne materiały metaliczne – teraźniejszość i przyszłość. Wydział Inżynierii Materiałowej Politechniki Śląskiej, Katowice 2009.
[3] Czuchryj J., Sikora S.: Niezgodności spawalnicze w złączach spawanych z metali i termoplastycznych tworzyw sztucznych. Instytut Spawalnictwa, Gliwice 2016.
[4] Honarvar F., Varvani-Farahani A.: A review of ultrasonic testing applications in additive manufacturing: Defect evaluation, material characterization and process control. Ultrasonics, 2020, vol. 108, 106227.
[5] Chang L.-S., Chuang T.-H., Wei W.J.: Characterization of alumina ceramics by ultrasonic testing, Material Characterization, 2000, vol. 45, no. 3, pp. 221-226.
[6] KRONOS EDM, PA11 (AW-5754), online: https://www.kronosedm.pl/aluminium-pa11-aw-5754, access date: 20.06.2022.
[7] Olympus, OmniScan MX2, online: https://www.olympus-ims.com/pl/omniscan-mx2, access date: 26.06.2022.